

# Generation of 40-GHz control signals from flag pulses for switching all-optical gates for use with optical packets

Konstantinos Yiannopoulos, Leontios Stampoulidis, Thanasis Houbavlis, and Hercules Avramopoulos

School of Electrical and Computer Engineering, National Technical University of Athens, Zografou, GR 15773 Athens, Greece

Received July 30, 2003

We demonstrate an all-optical circuit capable of generating 40-GHz control signals from flag pulses that can be used to define the switching state of all-optical gates for use with optical packets. The circuit comprises a Fabry–Perot filter and a semiconductor optical amplifier, and with a single pulse it can generate 12 control pulses with 0.64-dB amplitude modulation. With two and three flag pulses the number of control pulses becomes 36 and 54, respectively. © 2004 Optical Society of America

OCIS codes: 050.2230, 250.5980.

The past decade has been one of continuing advance in all-optical switching concepts and remarkable technological improvement, including the integration of all-optical interferometric switches that use semiconductor optical amplifiers (SOAs) as their switching elements.<sup>1</sup> A prime application of all-optical switching is in optical packet switching, which is considered the next step in the evolution of high-capacity optical fiber networks due to improvements in network performance and resource utilization.<sup>2,3</sup> The use of ultrahigh-bandwidth, all-optical, logical elements for on-the-fly signal processing directly in the optical domain can help eliminate optical–electrical–optical conversions in a switch and simplify its switching matrix and control algorithms. To this end, optically addressable  $2 \times 2$  switches<sup>4</sup> and circuits for recovering the optical clock from short packets<sup>5</sup> and separating the header from the payload<sup>6</sup> have recently been demonstrated.

However, to be able to use all-optical switches in an optical packet environment, one must generate a switch control signal locally from routing information embedded in the packet headers after header separation. All-optical interferometric switches are two logical state-switching elements, and each switch requires a single controlling bit to define its state per incoming data bit. If the incoming data signal is in the form of optical packets so that the complete packet must either be switched or not, the state of the switch must remain the same for the duration of the packet. Since for each switch a single controlling bit (or flag) is inserted in the packet header and since the switch-state controlling signal must persist for the duration of the packet, an optical circuit that can replicate the controlling bit as many times as the number of bits in the packet is therefore necessary. In this Letter we demonstrate for the first time to our knowledge such a circuit that can be used to generate the control signal from flag bits to operate optical gates at 40 GHz. We show that the control sequence may be extended with the use of repetitive flag bits, and we investigate the parameter choice for the circuit to operate at higher repetition rates.

The circuit comprises a Fabry–Perot (FP) filter arranged in a double-pass configuration followed by a SOA. The circuit takes advantage of the memory properties of the FP filter to generate a sequence of amplitude-decaying pulses at a repetition rate equal to the free spectral range of the filter selected to be equal to the desired line rate. The double-pass configuration for the filter assists in significantly increasing its lifetime and effective finesse.<sup>7</sup> The purpose of the SOA is to equalize the amplitude-modulated train at the output of the FP filter, and it is used as a nonlinear-gain device operated under moderate saturation. In this way the high-energy pulses saturate the SOA gain deeper and experience less gain than the low-energy pulses. As a result, the pulse-train amplitude modulation is minimized.

The experimental setup is shown in Fig. 1, and it consists of two subunits, the flag pulse generator and the control signal generator. The pulses used to generate the flag signal were obtained from a gain-switched distributed feedback laser operating at 1549.4 nm and yielding 40-ps pulses at 2.1882 GHz. This pulse train was modulated in a Ti:LiNbO<sub>3</sub> modulator with variable-width electrical pulses at 437.64 MHz to obtain the flag signal and so that one to four out of every five flag pulses could be selected. The flag pulses were then amplified in an erbium-doped fiber amplifier (EDFA1) and had their temporal width reduced in a fiber compressor. The fiber compressor consisted of a linear-compression stage comprising dispersion-compensating fiber of total negative dispersion equal to 55.58 ps/nm and a

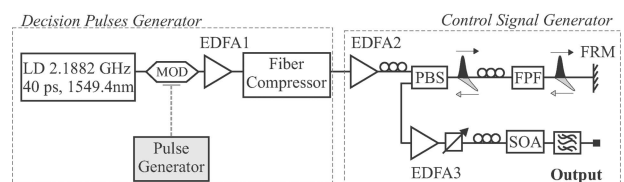


Fig. 1. Experimental setup: LD, laser diode; MOD, modulator; PBS, polarization beam splitter; FPF, Fabry–Perot filter; FRM, Faraday rotator mirror.

nonlinear-compression stage comprising alternating sections of dispersion-shifted and standard single-mode fiber and followed with a 1-nm pulse-shaping filter. After the linear-compression stage, the pulse width was reduced to 9 ps, and at the end of the nonlinear-compression stage it was reduced to 1.5 ps. The flag pulses were reamplified in EDFA2 to compensate for losses in the fiber compressor and were fed through the ordinary axis of a polarization beam splitter into a beam expander holding the FP filter. The FP filter was a dielectric film-coated, fused-quartz substrate with a free spectral range of 39.3876 GHz and a finesse of 50, which corresponds to a facet reflectivity of 0.939. A Faraday rotator mirror was used after the beam expander to effect the double-pass arrangement. The double-pass arrangement resulted in an enhanced finesse of 625, compared with the single-pass finesse of 50 for this FP filter, and was used because we lacked a filter with this high finesse. If a FP filter of appropriate finesse is available, the double-pass arrangement can be avoided to simplify the experimental setup. After it was passed twice through the FP filter, the resulting pulse stream exited through the extraordinary axis of the polarization beam splitter to a 90° polarization rotation at the Faraday rotator mirror and was further amplified in EDFA3. This signal was next introduced in a 1.5-mm-long, bulk SOA with a small signal gain of 24 dB at 1549.4 nm, 3-dB polarization gain dependence, and 65-ps gain recovery time when driven at 700 mA. The degree of gain saturation in the SOA and the polarization state at its input were adjusted with a variable optical attenuator and polarization controller, respectively. The output of the circuit was monitored after passing through a 1-nm filter.

Figure 2 shows the experimental results obtained from the circuit, monitored with a 40-GHz electrical input of a digital sampling oscilloscope, triggered at the flag rate. Figures 2(a), 2(b), and 2(c) record results when the circuit operates with one, two, or three flag pulses, respectively, with the multiple flag pulses separated by 2.28 ns. The upper, middle, and bottom rows correspond to the flag signal at the input of the FP filter, the signal after passing twice

through the FP filter, and the signal at the output of the SOA. When the circuit that generates the control pulse was operated with a single flag pulse, it generated a sequence of 12 pulses with amplitude modulation of less than 0.64 dB. This value of amplitude modulation is low and can be further reduced in all-optical interferometric gates due to their nonlinear transfer function.<sup>6</sup> With two and three decision or flag pulses the circuit generated sequences of 36 and 54 pulses, respectively, with amplitude modulation of less than 0.64 dB. Consequently, by doubling or tripling the number of flag pulses, the length of the generated sequence of control pulses increased by a factor of approximately 2 or 3. In all cases the generated signal rose from the third bit and had a  $1/e$  decay tail of approximately ten pulses. The sharp rise time is a result of gain saturation in the SOA, whereas the decay time is controlled by the effective FP filter lifetime. The average energy per pulse at the input of the SOA was 28 fJ. The 40-GHz trains of Figs. 2(b) and 2(c) show that there is no complete extinction from pulse to pulse. This is partly because of the low trigger frequency of the flag pulses (437.64 MHz) used and electrical jitter in the sampling oscilloscope and partly because of timing jitter accumulation in the fiber compressor. To verify that complete pulse-to-pulse extinction is achieved with the circuit, the output signal was triggered with the distributed feedback gain-switching signal at 2.1882 GHz, and the pulse waveforms were monitored without the nonlinear fiber compressor. Figure 2(d) shows the pulse waveforms obtained in this way and verifies complete pulse-to-pulse extinction.

The performance of the circuit was further investigated with a simulation tool based on the transfer function of the FP filter, the equations describing the saturation and recovery of the SOA,<sup>8</sup> and the experimental parameter values. The simulation tool was used to optimize the repetition rate of the flag pulses and the finesse of the FP filter against the resulting amplitude modulation at 40 GHz and to investigate its performance at 80 GHz. Figure 3(a) shows the amplitude modulation of the generated control pulses versus the repetition rate of the flag pulses for

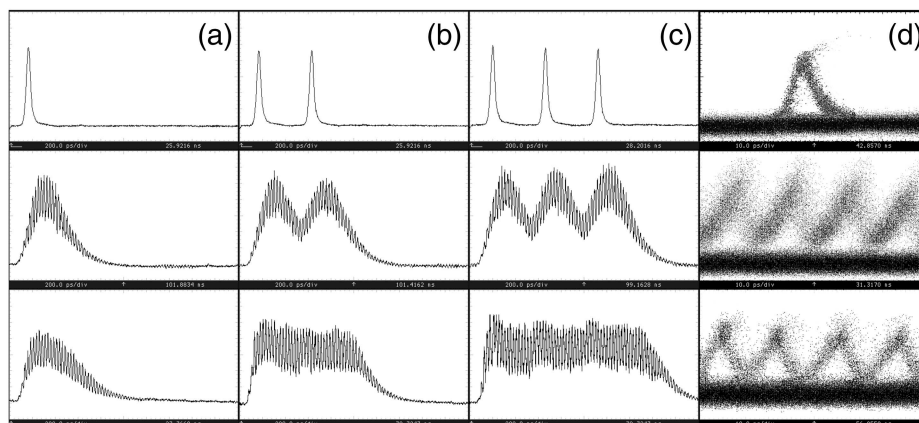


Fig. 2. Oscilloscope traces for (a) one, (b) two, and (c) three flags. The rows correspond to the flag pulses, the output of the double-pass FP filter, and the generated control signals at the output of the SOA. Time base is 200 ps/div. (d) Equivalent pulse waveforms. Time base is 10 ps/div.

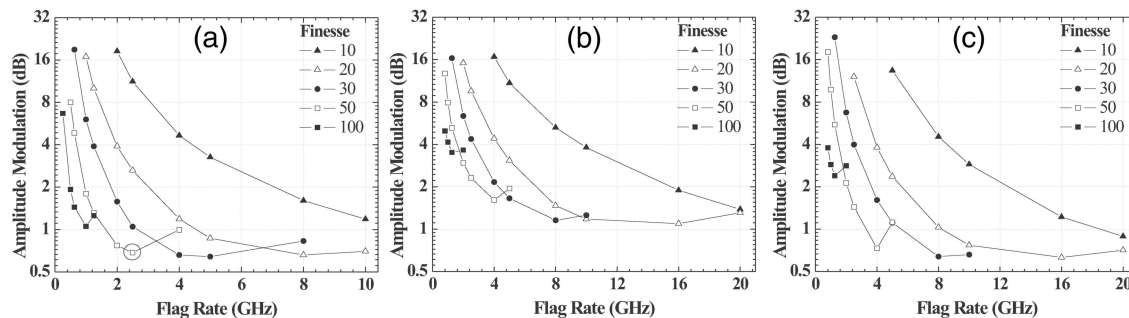


Fig. 3. Calculated amplitude modulation versus the flag repetition rate for several FP filter finesses when the line rate is (a) 40 GHz and (b) 80 GHz and a SOA with 65-ps recovery time is employed. The circle indicates the experimental point. (c) Same as (b), but with a SOA with a 20-ps recovery time.

different FP filter finesses at 40 GHz, and the point corresponding to the experimental setup is indicated by a circle. The figure shows that for each finesse value the amplitude modulation of the generated control signal goes through a minimum for a given rate of the flag pulses. However, because the input flag pulses represent an overhead on the available transmission bandwidth, their rate must be kept to a minimum. The performance of the circuit was also investigated at 80 GHz for optical signal processing applications at higher rates.<sup>9,10</sup> With the same SOA as before, the amplitude modulation at the output of the circuit was degraded by 0.5 dB, as shown in Fig. 3(b). This degradation can be overcome if the circuit uses a SOA with a faster recovery time, which is feasible by means of optical pumping<sup>11</sup> or by use of a quantum-dot SOA,<sup>12</sup> and Fig. 3(c) shows the simulated results for a SOA with 23-dB gain and 20-ps 10%–90% recovery time.

In conclusion, we have demonstrated a circuit capable of generating the control signal to drive all-optical gates so that they can be used with optical packets. The circuit can produce a sequence of control pulses from single or multiple pulses that would be embedded in the packet. The amplitude modulation of the generated control signal can be designed to be low, and in the present demonstration at 40 GHz it was less than 0.64 dB.

K. Yiannopoulos's e-mail address is kyianno@cc.ece.ntua.gr.

## References

1. K. E. Stubkjaer, *IEEE J. Sel. Top. Quantum Electron.* **6**, 1428 (2000).
2. D. J. Blumenthal, J. E. Bowers, L. Rau, H.-F. Chou, S. Rangarajan, W. Wang, and K. N. Poulsen, *IEEE Commun. Mag.* **41**, S23 (2003).
3. E. M. Varvarigos, *J. Lightwave Technol.* **16**, 1757 (1998).
4. G. Theophilopoulos, M. Kalyvas, C. Bintjas, N. Pleros, K. Yiannopoulos, A. Stavdas, H. Avramopoulos, and G. Guekos, *IEEE Photon. Technol. Lett.* **14**, 998 (2002).
5. C. Bintjas, K. Yiannopoulos, N. Pleros, G. Theophilopoulos, M. Kalyvas, H. Avramopoulos, and G. Guekos, *IEEE Photon. Technol. Lett.* **14**, 1363 (2002).
6. C. Bintjas, N. Pleros, K. Yiannopoulos, G. Theophilopoulos, M. Kalyvas, H. Avramopoulos, and G. Guekos, *IEEE Photon. Technol. Lett.* **14**, 1728 (2002).
7. K. Yiannopoulos, K. Vyrsoinos, E. Kehayas, N. Pleros, K. Vlachos, H. Avramopoulos, and G. Guekos, *IEEE Photon. Technol. Lett.* **15**, 1294 (2003).
8. M. Eiselt, W. Pieper, and H. G. Weber, *J. Lightwave Technol.* **13**, 2099 (1995).
9. K. L. Hall and K. A. Rauschenbach, *Opt. Lett.* **23**, 1271 (1998).
10. S. Nakamura, Y. Ueno, and K. Tajima, in *Optical Fiber Communication (OFC)*, Vol. 70 of OSA Trends in Optics and Photonics Series (Optical Society of America, Washington, D.C., 2002), pp. FD3.1–FD3.3.
11. R. J. Manning, D. A. O. Davies, S. Cotter, and J. K. Lucek, *Electron. Lett.* **30**, 787 (1994).
12. O. Qasimeh, *IEEE J. Quantum Electron.* **39**, 793 (2003).